Pharmaceutical Research, Vol. 26, No. 3, March 2009 (© 2008)
DOI: 10.1007/s11095-008-9770-5

Research Paper

Reduced Antidiabetic Effect of Metformin and Down-regulation of Hepatic Oct1 in Rats with Ethynylestradiol-Induced Cholestasis

Hyo-Eon Jin,[1] Soon-Sun Hong,[3] Min-Koo Choi,[1] Han-Joo Maeng,[2] Dae-Duk Kim,[2] Suk-Jae Chung,[2] and Chang-Koo Shim[1,2,4]

Received August 28, 2008; accepted October 28, 2008; published online November 11, 2008

Purpose. To investigate the effect of 17α-ethynylestradiol (EE)-induced cholestasis on the expression of organic cation transporters (Octs) in the liver and kidney, as well as the pharmacokinetics and pharmacodynamics of metformin in rats.
Methods. Octs mRNA and protein expression were determined. The pharmacokinetics and tissue uptake clearance of metformin were determined following *iv* administration (5 mg/kg). Uptake of metformin, glucagon-mediated glucose production, and AMP-activated protein kinase (AMPK) activation were measured in isolated hepatocytes. The effect of metformin (30 mg/kg) on blood glucose levels was tested using the *iv* glucose tolerance test (IVGTT).
Results. The mRNAs of hepatic Oct1, renal Oct1, and Oct2 were decreased by 71.1%, 37.6%, and 94.5%, respectively, by EE cholestasis. The hepatic Oct1 and renal Oct2 proteins were decreased by 30.6% and 60.2%, respectively. The systemic and renal clearance of metformin were decreased. The *in vitro* hepatocyte uptake of metformin was decreased by 86.4% for V_{max}. Suppression of glucagon-stimulated glucose production and stimulation of AMPK activation in hepatocytes by metformin were diminished. In addition, metformin did not demonstrate a glucose-lowering effect during IVGTT in EE cholestasis.
Conclusion. The antidiabetic effect of metformin may be diminished in diabetic patients with EE cholestasis, due to impaired hepatic uptake of the drug *via* OCT1.

KEY WORDS: antidiabetics; cholestasis; metformin; organic cation transporter; 17α-ethynylestradiol.

INTRODUCTION

Biguanide metformin (Fig. 1) is widely used as a first-line therapy for the treatment of type 2 diabetes (1). It was developed during the late 1950s, was first marketed in Europe in 1959, and has been available in the US since 1995 (2). Metformin ameliorates hyperglycemia by reducing gastrointestinal glucose absorption and hepatic glucose production, and by improving glucose utilization (1). Molecular mechanisms underlying metformin action appear to be related to its activation (phosphorylation) of the energy sensor, AMP-activated protein kinase (AMPK), which suppresses glucagon-stimulated glucose production and causes an increase in glucose uptake in muscle and hepatic cells (3,4). Serine-threonine kinase 11 (STK11/LKB1), which phosphorylates AMPK, also is reportedly involved in the effects of metformin (5,6).

Recently, metformin has been found to improve vascular function (7), reverse fatty liver disease in obese mice (8), prevent pancreatic cancer (9), and it has been used with oral contraceptives for the treatment and/or prevention of polycystic ovary syndrome (10). In addition, although the use of metformin is not yet accepted, evidence is accumulating that it may be a useful treatment for gestational diabetes (11). In gestational diabetes, treatment with additional insulin for persistent maternal hyperglycemia has been shown to improve perinatal outcomes. However, the use of insulin is also associated with hypoglycemia and weight gain, suggesting that the use of safe and effective oral hypoglycemic agents may offer advantages over insulin. Metformin may be a feasible option for the treatment of gestational diabetes, because it improves insulin sensitivity and is not associated with weight gain or hypoglycemia (1,12).

Estrogen has long been known to cause intrahepatic cholestasis in susceptible women during pregnancy (0.5–1.8% of pregnant women suffer from intrahepatic cholestasis, (13–15),

[1] National Research Laboratory for Transporters Targeted Drug Design, Research Institute of Pharmaceutical Sciences, College of Pharmacy, Seoul National University, 599 Gwanangno, Gwanak-gu, Seoul, 151-742, Republic of Korea.
[2] Research Institute of Pharmaceutical Sciences, College of Pharmacy, Seoul National University, Seoul, Republic of Korea.
[3] Center for Advanced Medical Education (BK21), Inha University School of Medicine, Incheon, Republic of Korea.
[4] To whom correspondence should be addressed. (e-mail: shimck@snu.ac.kr)

ABBREVIATIONS: AMPK, AMP-activated protein kinase; AUC, area under the plasma concentration time curve; Bsep, bile salt export pump; EE, 17α-ethynylestradiol; Mrp, multidrug resistance associated protein; Ntcp, sodium-dependent taurocholate cotransporter; Oatp, organic anion transporter; Oct, organic cation transporter; RT-PCR, reverse transcription-polymerase chain reaction; IVGTT, intravenous glucose tolerance test; r, rat.

0724-8741/09/0300-0549/0 © 2008 Springer Science + Business Media, LLC

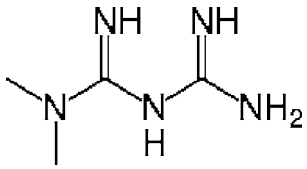

Fig. 1. Chemical structure of metformin.

after the administration of oral contraceptives, or during postmenopausal hormone replacement therapy (16). Experimental intrahepatic cholestasis induced by 17α-ethynylestradiol (EE) is a widely used *in vivo* animal model used to examine the molecular mechanisms involved in estrogen-induced cholestasis (17). In EE-induced cholestasis, the expression of transporters is generally reduced in association with impaired biliary secretory function. For example, EE-induced a reduction in ATP-dependent transport of taurocholate by canalicular vesicles (18), and decreased expression of the bile salt export pump (Bsep [Abcb11]) (19) and multidrug resistance associated protein 2 (Mrp2 [Abcc2]) (20,21). Induced expression of basolateral multidrug resistant protein 3 (Mrp3 [Abcc3]) by EE may represent a compensatory mechanism to prevent intracellular accumulation of common Mrp substrates, either endogenous or exogenous, due to reduced expression and activity of apical Mrp2. (22). Basolateral sodium/taurocholate cotransporter, (Ntcp [Slc10a1]), organic anion transporter 1 (Oatp1 [Slco1a1]), Oatp2 [Slco1a4], and Oatp4 [Slco1b2] were also down-regulated at the protein level in EE-induced cholestasis (23). However, P-gp was not impaired (24).

Metformin is the substrate of organic cation transporters 1 and 2 (OCT1 and OCT2) (25,26). Recently, genetic polymorphisms in OCT1 and OCT2 have been found to be associated with changes in the pharmacokinetic and pharmacodynamic responses to metformin (27,28). The purpose of the present study, therefore, was to determine the effects of EE-induced cholestasis on the expression of Oct1 and Oct2 in the liver and kidney, and subsequently on the pharmacokinetics and pharmacodynamics of metformin.

MATERIALS AND METHODS

Materials

1,1-dimethylbiguanide hydrochloride (metformin), 17α-ethynylestradiol (EE), antipyrine, 1,2-propanediol, bicinchoninic acid, glucagon, pyruvate, and L-lactate were purchased from Sigma-Aldrich (St. Louis, MO, USA). [^{14}C]-metformin hydrochloride (specific activity 112 mCi/mmol) was purchased from Moravek Biochemicals, Inc. (Brea, CA, USA).

Animals

Male Sprague-Dawley rats (Orient Bio Inc., Seong-Nam, Korea), weighing 240–290 g, were used in this study. All rats were maintained on water and a standard diet and were housed in a temperature- (20–23°C) and humidity-controlled (50–60%) room under a constant 12 h light/dark cycle. All animal experiments were performed according to the Guidelines for Animal Care and Use, Seoul National University.

Induction of Intrahepatic Cholestasis in Rats by 17α-Ethynylestradiol Administration

Intrahepatic cholestasis was induced by the daily subcutaneous injection of 17α-ethynylestradiol (EE) in 1,2-propanediol (10 mg/kg) for five consecutive days. Control rats were injected daily with 1,2-propanediol alone. All studies were performed at 24 h after the last administration of EE.

Cholestatic Parameters

The degree of EE-induced cholestasis was estimated by the determination of bile acids, alkaline phosphatase, and testosterone in serum (analyzed by Green Cross Reference Laboratory, Seoul, Korea). For bile flow estimation, the common bile duct of the rats was cannulated using polyethylene 10 tubing. After a 30 min collection of the bile juice in the EP tube, the mean bile flow was estimated gravimetrically, assuming a bile solution density of 1.0. The rats were euthanized, and the liver and kidney were excised and fixed with 4% neutral buffered formaldehyde solution. Paraffin sections were then stained with hematoxylin and eosin, and light microscopy of liver and kidney specimens was conducted.

Pharmacokinetics of Metformin in Rats

Control and EE cholestatic rats were anesthetized with ketamine (45 mg/kg, *im*) and acepromazine (5 mg/kg, *im*) and the femoral artery and vein were cannulated with a polyethylene tube (PE-50; Clay Adams, Parsippany, NJ, USA) filled with heparinized saline (20 IU/ml) to prevent blood clotting. After recovery from the anesthesia, the rats were intravenously administered metformin at a dose of 5 mg/kg. Blood samples were taken from the femoral artery cannula of each rat at 0, 1, 3, 5, 10, 30, 60, 90, and 120 min after metformin administration. The blood volume withdrawn at each time point was replaced with an equal volume of saline to compensate for fluid loss. The plasma samples were separated by centrifugation and stored at −80°C until HPLC analysis. Briefly, for the analysis of plasma samples, an aliquot of 100 μl of the sample was spiked with 20 μl of internal standard acetonitrile solution (antipyrine, 50 μg/ml) and 180 μl acetonitrile and mixed. The mixture was then centrifuged and evaporated to dryness. Pellets were dissolved in 200 μl of DDW for HPLC analysis. 100 μl of the supernatant was injected for HPLC analysis.

The area under the plasma concentration–time curve from zero to infinity (AUC) was calculated by the trapezoidal-extrapolation method (29). For extrapolation, the area from the last datum point to time infinity was estimated by the terminal-phase rate constant. Standard methods (30) were used to calculate the time-averaged total body clearance (CL), renal (CL_R) and nonrenal (CL_{NR}) clearance, and the apparent volume of distribution at steady state (V_{dss}) by a non-compartmental analysis using WinNonlin® 3.1 (Pharsight Co., Mountain View, CA, USA).

The glomerular filtration rate (GFR) was estimated by calculating the creatinine clearance (CL_{cr}), assuming that the kidney function was stable during the experimental period. The CL_{cr} was calculated by dividing the total amount of unchanged creatinine excreted in urine over 24 h by the $AUC_{0-24\ h}$ of creatinine in plasma.

In Vivo Tissue Uptake Clearance

The early-phase tissue uptake clearance (CL_{uptake}) by the liver or kidney was determined *in vivo* within 3 min after the *iv* administration of metformin. Rats were anesthetized with ketamine and acepromazine and the femoral artery and vein were cannulated with a polyethylene tube (PE-50; Clay Adams, Parsippany, NJ, USA), filled with heparinized saline (20 IU/ml). Metformin (5 mg/kg) was intravenously administrated to control and EE cholestatic rats, and blood samples were collected at 0, 0.5, 1, 2, 3 min. The animals were sacrificed at 3 min after the administration of metformin, and the liver and kidney were immediately dissected. Tissues were weighed and homogenized with one volume of PBS. A 100 μl aliquot of both homogenized tissues and blood samples was spiked with 20 μl of internal standard acetonitrile solution (i.e., 50 μg/ml of antipyrine) and 180 μl acetonitrile, and mixed. The mixture was then centrifuged and evaporated to dryness. The resulting pellets were dissolved in 200 μl of DDW for HPLC analysis. One hundred microliters of the supernatant was injected for HPLC analysis. *In vivo* uptake clearance, CL_{uptake}, was estimated using Eq. 1, where $X_{3\ min}$ represents the amount of metformin in the tissue at 3 min and $AUC_{0-3\ min}$ represents the area under the curve up to 3 min.

$$CL_{\text{uptake}} = X_{3\text{min}}/AUC_{0-3\text{min}} \quad (1)$$

Plasma Protein Binding Study

The plasma protein binding of metformin in control and EE cholestatic rats was determined by ultrafiltration using Amicon centrifuge micropartition devices (Centricon, Amicon, Millipore Corporation, Bedford, MA, USA). Plasma was incubated in the presence of 10 μg/ml metformin at 37°C for 12 min. After incubation, 100 μl of aliquot was taken for the determination of total plasma concentration. The plasma was then placed in an ultrafiltration apparatus and centrifuged at 5,000 rpm for 12 min. After centrifugation, the concentration in the filtrate was determined as the unbound concentration. The concentration of metformin was determined by HPLC analysis according to the method mentioned above.

HPLC Analysis

The concentration of metformin was determined by the modified reversed-phase HPLC method (26). The HPLC system involved a Waters 717 plus autosampler, a 515 HPLC dual pump, and a 2487 Dual λ absorbance detector (Milford, MA, USA). The HPLC was performed using a C_{18} μBondapak (150×3.9 mm i.d. 10 μm, Waters, Milford, MA, USA). The mobile phase consisted of 10 mM phosphate buffer containing 10 mM sodium dodecyl sulfate (pH 7) and acetonitrile (65:35). The flow rate of the mobile phase was 1 ml/min, and the wavelength of the UV detection was 236 nm.

Real-time RT-PCR Analysis

The Oct mRNA expression in liver (Oct1 [slc22a1]) and kidney (Oct1 and Oct2 [slc22a2]) was examined in control (n=4) and EE cholestatic rats (n=4). Total RNA was extracted from the liver and kidney tissues using TRIzol reagent (Invitrogen, Carlsbad, CA, USA) according to the standard protocol. The concentration and purity of the RNA were determined by spectrophotometry. Reverse transcription was performed on 1 μg of isolated rat total RNA using the RNA LA PCR kit Ver. 1.1 (Takara Shuzo Co., Ltd., Shiga, Japan). Quantitative real-time PCR was performed on the LightCycler 1.5 system (Roche Applied Science, Indianapolis, IN, USA) using the FastStart DNA Master^{PLUS} SYBR Green Kit (31), according to the protocol (Roche Applied Science, Indianapolis, IN, USA). Primers specific for Mrp2, Oct1, Oct2, and β-actin (as the reference) were all designed by Perfect Real-time Support System (Takara Bio, Takara Shuzo Co., Ltd., Shiga, Japan). The cycling conditions were carried out as follows: initial denaturation at 95°C for 6 min, followed by 40 cycles of denaturation at 95°C for 15 s, annealing at 59°C for 5 s and extension at 72°C for 10 s. To distinguish the specific amplification product from non-specific products or primer dimers, a melting curve was constructed from the amplification reaction obtained by maintaining the temperature at 65°C for 15 s, followed by a gradual temperature increase rate of 0.1°C/s to 95°C. For this study, the signal acquisition mode was set at continuous.

Western Blot Analysis of Octs

Western blot analysis was performed to determine the levels of Oct1 in the liver and Oct1 and Oct2 in the kidney. Liver and kidney (n=4) were homogenized in ice-cold cell lysis buffer (Cell Signaling Technology, Beverly, MA, USA) containing protease inhibitors (Complete® protease inhibitor cocktail tablet, Roche Diagnostics, Mannheim, Germany). The homogenate was centrifuged at 3,000×g for 10 min, and the membrane fraction pellet was obtained from the supernatant after centrifugation at 100,000×g for 1 h at 4°C. The pellet was resuspended in the lysis buffer. The protein concentration was determined using the bicinchoninic acid (BCA) assay and samples were stored at −80°C. Aliquots of liver total membrane (45 μg) and kidney total membrane (40 μg) were separated with 10% sodium dodecyl sulfate (SDS)-polyacrylamide gel electrophoresis. The blotting membrane was blocked with phosphate-buffered saline containing 0.1% Tween 80 and 5% skim milk or BSA for 1 h at room temperature. The blots were washed and then incubated overnight at 4°C with polyclonal primary antibody (1:1,000) of anti-rOct1 or anti-rOct2 (Alpha Diagnostic Int., San Antonio, TX, USA). The bound antibody was visualized on X-ray film by chemiluminescence detection, using a secondary antibody coupled to horseradish peroxidase (Pierce Chemical, Rockford, IL, USA).

In Vitro Uptake into Hepatocytes

Primary hepatocytes were isolated from control and EE cholestatic rats using the standard collagenase method (32). The cell suspension (2 ml, 3×10^6 cells per milliliter) was preincubated on the medium for 5 min at 37°C. An aliquot of a [^{14}C]metformin solution was added to the suspension to give a final medium concentration of 5–1,000 μM (0.1 μCi/ml). An aliquot (200 μl) of the suspension was sampled at 20, 40, 60 and 90 s. The amount of substrates in the hepatocytes was plotted against time. The initial rate of uptake of the

metformin into the hepatocyte, which was calculated from the linear portion of the plot, was then plotted against the initial concentration of the substrate on the medium. A nonlinear regression analysis was performed on the fit of the plot to the following equation, using WinNonlin® 3.1.

$$V_0 = V_{max} \cdot S/(K_m + S) + CL_{linear} \cdot S \quad (2)$$

V_0 is the initial uptake rate of the metformin (pmol/min/10^6 cells), S is the concentration of metformin in the medium (μM). V_{max} and K_m are the maximum uptake rate and the medium concentration at half maximal rate, respectively, and CL_{linear} represents the linear uptake clearance.

Hepatocyte Glucose Production

Glucose production in primary hepatocytes was measured by modifying a previously described method (3). Primary cultures of hepatocytes from control and EE cholestatic rats were incubated at 37°C at 4×10^6 cell per milliliter in bicarbonate-buffered saline medium containing 10 mM L-lactate, 1 mM pyruvate, and 0.3 μM glucagon, with a gas phase of O_2/CO_2 (19:1), with or without 2 mM metformin for 180 min. Glucose was measured using Accu-CHEK® Sensor Comfort Glucose (Roche Diagnostics GmbH, Germany).

Primary hepatocyte samples were homogenized for 30 min in ice-cold lysis buffer containing 50 mM NaF with protease inhibitors (Complete® protease inhibitor cocktail tablet, Roche Diagnostics, Mannheim, Germany). After centrifugation at 14,000×*g* for 10 min at 4°C, the supernatants were removed in order to determine the protein content and perform Western blot analysis. Forty micrograms of proteins from the supernatant were separated by SDS gel electrophoresis. Primary antibodies were directed against AMPKα, AMPKα phosphorylated at Thr172, and β-actin (all from Cell Signaling Technology, MA, USA).

Intravenous Glucose Tolerance Test

Control and EE cholestatic rats were fasted overnight (18 h) prior to the IVGTT. The carotid artery and the jugular vein of each rat were cannulated with a polyethylene tube under light ether anesthesia. Each rat was housed individually in a metabolic cage (Daejong Scientific Co., Seoul, Korea) and allowed to recover from anesthesia for 3–4 h prior to the experiment. A baseline blood sample was collected through a carotid artery cannula. The rats were administered metformin (30 mg/ml/kg) or the equivalent volume of saline intravenously. After 1 min, glucose (40% D-glucose, 1 g/kg) was injected intravenously, then blood samples were collected at 1, 5, 10, 20, 30, 45, and 60 min after the glucose administration. The change in plasma glucose concentration (Δ Plasma Glucose Concentration=plasma glucose concentration during IVGTT−baseline plasma glucose concentration) after the glucose treatment in the control and EE cholestasis groups was compared (27,33). The area under the curve ($AUC_{0-60\ min}$) of Δ Plasma Glucose Concentration in each rat during IVGTT was calculated using WinNonlin® 3.1. Glucose was measured using Accu-CHEK® Sensor Comfort Glucose.

Statistical Data Analysis

All *in vivo* and *in vitro* data are presented as mean±SD for all experiments. When it was necessary to compare the means between treatments, an unpaired Student's *t*-test was applied to analyze the data. A *P* value of less than 0.05 was considered significant.

RESULTS

Induction of Cholestasis

In this study, intrahepatic cholestasis was induced by the daily subcutaneous injection of EE for five consecutive days; control rats were injected with the vehicle only. The body weight of the rats was monitored over the 6 days of the experimental period for both control and EE cholestatic rats. EE-treated rats had lower body weight compared with control rats at day 6 (Table I). The body weight of the control rats increased continuously during the experimental period, while the body weight of the EE cholestatic rats decreased during the same period. Liver weight increased, but bile flow was reduced by cholestasis (Table I). In addition, serum alkaline phosphatase and bile acids were significantly increased, but testosterone level was decreased by EE cholestasis (Table I). Light microscopy of liver specimens found damage as previously reported (34,35), but no significant findings were detected in the kidneys of any group of rats (data not shown). These observations suggest that EE administration led to experimental cholestasis in this study.

Pharmacokinetics of Metformin in Rats

Mean plasma concentration–time profiles of metformin in control and EE cholestatic rats are shown in Fig. 2, and pharmacokinetic parameters are summarized in Table II. The plasma concentrations of metformin in the EE cholestatic rats were significantly higher for the initial 5 min period after the drug administration. As a result, the area under the plasma concentration–time curve (AUC) was increased 1.3-fold by EE cholestasis. The systemic clearance (CL) and renal clearance (CL_R), but not the nonrenal clearance (CL_{NR}), were significantly decreased by EE cholestasis. However, creatinine clearance (CL_{CR}) did not differ significantly between the control and the EE cholestatic rats, suggesting that the CL_R decrease was not associated with impairment of

Table I. Characteristics of Control and EE Cholestatic Rats

Parameters	Control	EE cholestasis
Initial body weight (g)	269.0±3.7	274.5±3.1
Final body weight (g)	296.0±2.4	242.4±7.8**
Liver weight (g)	10.4±0.9	13.1±0.9*
Bile flow (μl/min/g liver)	2.6±0.6	1.2±0.1*
Serum		
Alkaline phosphatase (U/L)	187±38.8	331±26.1*
Bile acids (μmol/L)	13.3±2.1	39.1±7.5*
Testosterone (ng/ml)	1.6±0.2	0.08±0.04**

Each value represents the mean±SD, $n=4$
*$p<0.05$; **$p<0.001$ from the control group by Student's *t*-test

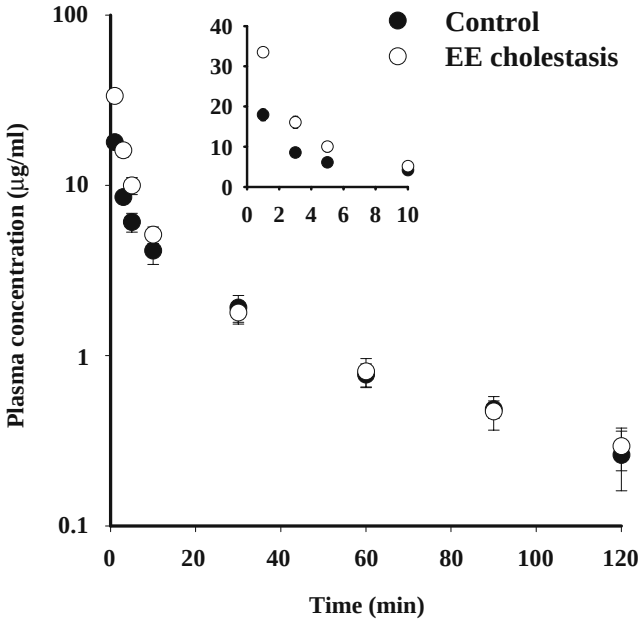

Fig. 2. Plasma concentration profile of metformin in control (*filled circles*) and EE cholestatic rats (*empty circles*). Metformin was injected intravenously at 5 mg/kg. Each data point represents the mean±SD for four rats.

the glomerular filtration rate. The distribution of the drug at a steady state (V_{dss}) was decreased 0.57-fold by EE cholestasis.

In Vivo Tissue Uptake Clearance of Metformin

In vivo tissue uptake data are summarized in Table III. Due to the decreased amount of the drug ($X_{3\ min}$) taken up by the liver and kidney under increased plasma AUC ($AUC_{0-3\ min}$) for the initial 3 min period, the uptake clearance (CL_{uptake}) for the liver and kidney was decreased to 28% and 62%, respectively, by EE cholestasis.

Plasma Protein Binding of Metformin

Metformin binding to plasma proteins was negligible, and there was no difference between experimental groups (8.4±0.91% and 9.5±1.9% for control and EE cholestatic rats, respectively, mean±SD, n=4).

Table II. Pharmacokinetic Parameters of Metformin after Intravenous Injection, at a Dose of 5 mg/kg, into Control and EE Cholestatic Rats

Parameter	Control	EE cholestasis
AUC (μg·min/ml)	235.5±22.7	297.3±36.2*
CL (ml/min/kg)	21.4±2.0	17.0±2.1*
CL_R (ml/min/kg)	17.6±2.5	13.5±0.3*
CL_{NR} (ml/min/kg)	3.9±1.2	3.3±0.6
V_{dss} (ml/kg)	766±180	434±43.7*
CL_{CR} (ml/min/kg)	3.72±0.38	3.69±0.55

Each value represents the mean±SD, n=4
*p<0.05 from the control group by Student's t-test

Table III. Distribution of Metformin after Intravenous Injection, at a Dose of 5 mg/kg, into Control and EE Cholestatic Rats

	Control	EE cholestasis
Plasma		
$AUC_{0-3\ min}$ (μg·min/ml)	63.4±9.8	85.4±1.9*
Liver		
$X_{3\ min,\ liver}$ (μg/g liver)	28.6±2.2	11.4±1.2***
$CL_{uptake,\ liver}$ (ml/min/g liver)	0.46±0.07	0.13±0.02*
Kidney		
$X_{3\ min,\ kidney}$ (μg/g kidney)	119.6±22.8	99.1±14.0
$CL_{uptake,\ kidney}$ (ml/min/g kidney)	1.88±0.11	1.16±0.19**

Each value represents the mean±SD, n=3
*p<0.05; **p<0.01, ***p<0.001 from the control group by Student's t-test

Real-time RT-PCR Analysis

Results of the real-time RT-PCR analysis are summarized in Fig. 3. mRNA levels for hepatic Oct1, renal Oct1, and renal Oct2 were decreased, after normalization for the mRNA level of β-actin (a reference marker), by cholestasis to 28.9±6.2%, 62.4±12.5% and 5.5±1.2% of their respective control values (Fig. 3A,B). The Mrp2 mRNA expression in the liver was decreased by EE cholestasis (47.4±6.4% of the control, Fig. 3A), which is consistent with previous reports (20,21).

Western Blot Analysis of Octs

Consistent with the results for mRNA (Fig. 3A), the density of the hepatic Oct1 band was decreased by EE cholestasis (Fig. 4A), indicating the expression of Oct1 in the liver decreased to 69.4±14.6% of the control value (Fig. 4B). The expression level of Oct2 protein in the kidney was also decreased by EE cholestasis (i.e., 39.8±22.9% of the control, Fig. 5A,B), consistent with the result for the corresponding mRNA (Fig. 3B). Despite the significant decrease in the level of mRNA for renal Oct1 (Fig. 3B), the protein level of renal Oct1 was not decreased significantly by EE cholestasis (100±16.3% and 82.6±14.6%, Fig. 5A,B).

In Vitro Uptake of Metformin into Hepatocytes

The effect of EE cholestasis on the metformin uptake into hepatocytes was measured *in vitro*. The temporal uptake profiles were apparently linear for 90 s for both control and EE cholestatic hepatocytes (data not shown). The plots of the initial uptake rates (velocity, V_0), which were represented by the slopes of the lines *vs.* the initial substrate concentrations (S), exhibited curvilinear relationships for both control and EE cholestatic hepatocytes (Fig. 6). The uptake rate of metformin into hepatocytes could be fitted to a saturable and a nonsaturable component (Fig. 6). The results of the nonlinear regression analysis of the data according to Eq. 2 are summarized in Table IV. A significant decrease in V_{max} (13.6% of control) was observed for EE cholestatic hepatocytes. However, no significant changes were observed in K_m and passive diffusion clearance (CL_{linear}) with EE cholestasis.

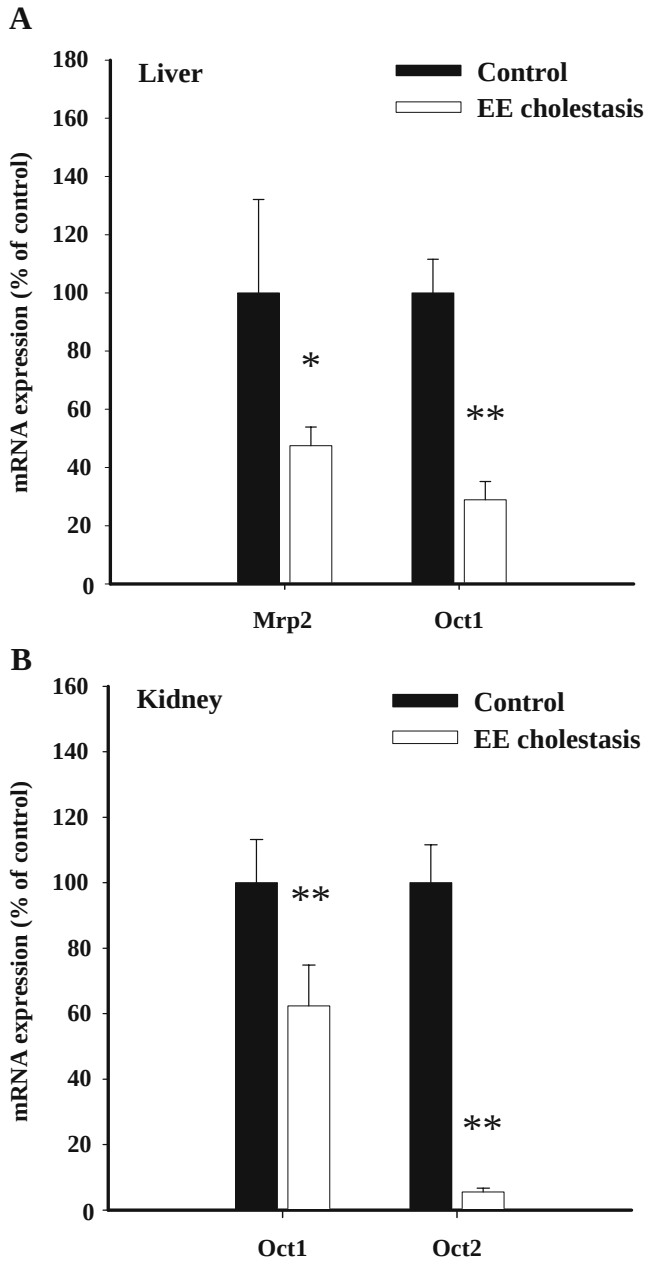

Fig. 3. mRNA expression of Mrp2, Oct1 and Oct2 by quantitative RT-PCR analysis in the liver (**A**) and kidney (**B**) of control and EE cholestatic rats. Data shown correspond to transporter mRNA levels and are expressed as a percentage of those found in control rats. *$p<0.05$, **$p<0.001$ from the control group by Student's *t*-test. The data are expressed mean±SD of approximately four to six rats.

As a result, the intrinsic clearance (CL_{int}, i.e., V_{max}/K_m) for carrier-mediated uptake was decreased to 12.5%, consistent with reduced expression of hepatic Oct1 (Fig. 4) with EE cholestasis (i.e., 2.63 vs 0.33 μl/min per 10^6 cells).

Hepatocyte Glucose Production

OCT1-mediated hepatic uptake of metformin appears to play a key role in determining one of the major pharmacologic effects of the drug (i.e., inhibition of hepatic gluconeogenesis) (27). Therefore, the relationship between the hepatic uptake of metformin in EE cholestasis and the effect of the drug on hepatic gluconeogenesis was investigated *in vitro* (Fig. 7). In control and EE cholestatic hepatocytes, glucagon-stimulated glucose production, increasing the glucose concentration in the medium in the absence of metformin (filled circles in Fig. 7A,B). The production of glucose was significantly suppressed (40%) by the presence of 2 mM metformin in control hepatocytes for a 180 min period (open circles in Fig. 7A), consistent with the pharmacological effect of metformin (i.e., glucose lowering effect). It is interesting that this effect of metformin (2 mM) was not observed for EE cholestatic hepatocytes (open circle in Fig. 7B).

Results of Western blot analysis for phosphorylation levels of AMPK (p-AMPK) in hepatocytes after the glucose production study are shown in Fig. 7C. Consistent with the above results (Fig. 7A,B), the level of p-AMPK was increased by the metformin treatment in control hepatocytes, but not in the EE cholestatic hepatocytes, suggesting that metformin no longer promoted AMPK activation (i.e., inhibition of hepatic glucose production). The levels of AMPK and β-actin did not differ between the treatments.

Intravenous Glucose Tolerance Test

The *in vivo* effect of metformin on blood glucose levels was investigated during the IVGTT in control and EE cholestatic rats. Δ Plasma Glucose Concentration was decreased

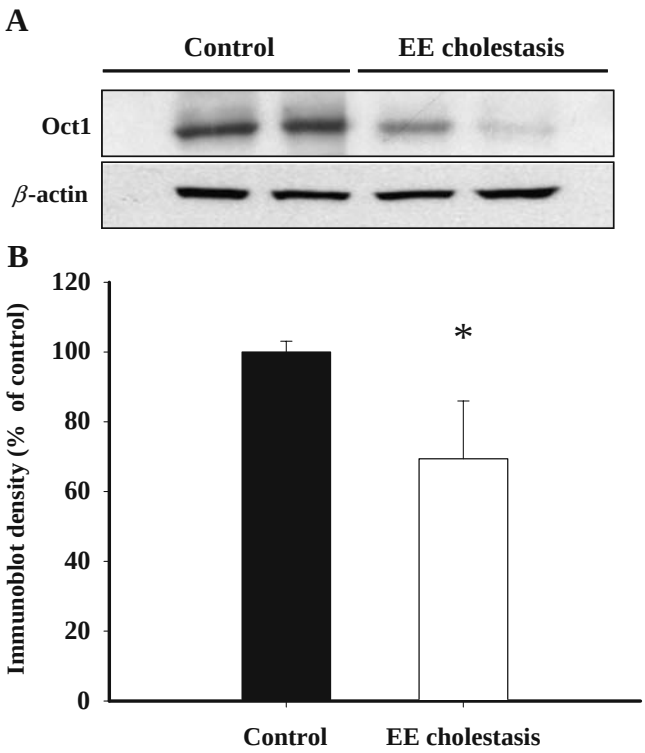

Fig. 4. Protein expression of Oct1 in the liver of control and EE cholestatic rats. **A** Representative Western blot. **B** Results of Oct1 protein expression represent the normalized (i.e., with the band density for β-actin) densitometry in the liver of control and EE cholestatic rats. Data are expressed as a percentage of control value (mean±SD, $n=4$). *$p<0.05$ from the control group by Student's *t*-test.

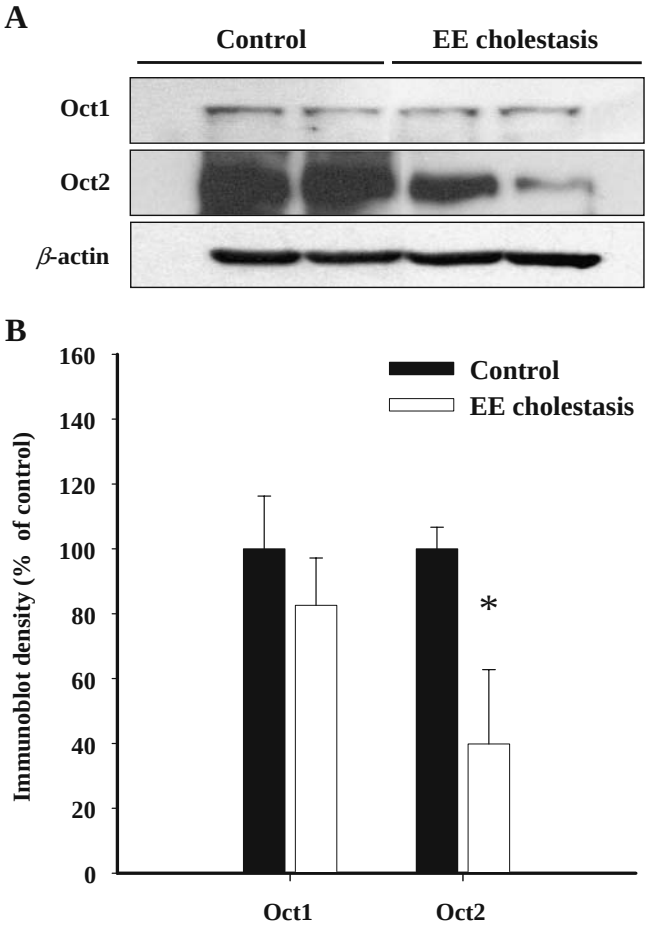

Fig. 5. Protein expression of Oct1 and Oct2 in the kidney of control and EE cholestatic rats. **A** Representative Western blot. **B** Results of densitometry of Oct1 and Oct2 protein expression in the kidney of control and EE cholestatic rats. Data are expressed as a percentage of control (mean±SD, $n=4$). *$p<0.001$ from the control group by Student's *t*-test.

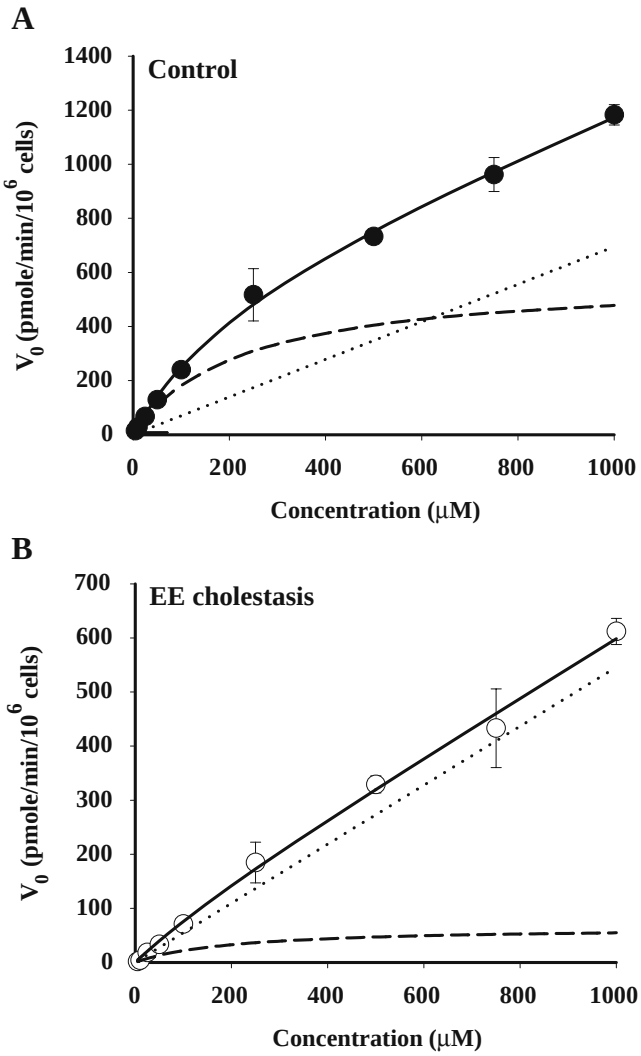

Fig. 6. Concentration dependency for the uptake of metformin by isolated hepatocytes from control (**A**, *filled circles*) and EE cholestatic rats (**B**, *empty circles*). The concentrations of metformin in the uptake studies were 5, 10, 25, 50, 100, 250, 500, 750, 1,000 μM. The transport of metformin into hepatocytes is shown with the fitted lines for the uptake data (*solid*), saturable (*dashed*), and nonsaturable (*dotted*) components, respectively. Fitted lines were generated using mean uptake parameters in Table IV. Each *point* and *vertical bar* represents the mean±SD of three experiments.

until 60 min after glucose administration in control and EE cholestatic rats (i.e., without metformin pretreatment; Fig. 8A). No significant differences in Δ Plasma Glucose Concentration or the mean AUC of the concentration were observed between control and EE cholestatic rats under these conditions (e.g., 75.1±5.38 and 81.1±4.81 mg/min per milliliter of AUC for control and EE cholestatic rats, Fig. 8A). The Δ Plasma Glucose Concentration of control rats was significantly lowered only by the metformin treatment (30 mg/kg) for 10–45 min post-glucose injection period, but in EE cholestatic rats, no significant differences in the Δ Plasma Glucose Concentration as a result of the metformin treatment were observed (Fig. 8B). As a result, the mean AUC of the Δ Plasma Glucose Concentration was significantly lower for control rats compared to cholestatic rats (64.7±7.71 and 94.3±18.8 mg/min per milliliter, $p<0.05$). This suggests that metformin (30 mg/kg) has no glucose level lowering effect during IVGTT in EE cholestatic rats, which is consistent with the results in Fig. 7. No significant differences in Δ Plasma Glucose Concentration or the mean AUC of the concentration were observed among control, EE cholestatic rats and EE cholestatic rats with metformin.

DISCUSSION

A number of drugs and physiological substances are classified as organic cations that are transported by organic

Table IV. *In vitro* Kinetic Parameters for Metformin Uptake by Control and EE Cholestatic Rats Hepatocytes

	Control	EE cholestasis
K_m (μM)	222.0±19.6	206.3±13.0
V_{max} (pmol/min/10^6 cells)	584.3±118.8	79.4±28.4*
CL_{int} (μL/min/10^6 cells)	2.63±0.48	0.33±0.19*
CL_{linear} (μL/min/10^6 cells)	0.69±0.10	0.53±0.05

Each value represents the mean±SD, $n=3$; CL_{int}, intrinsic clearance was calculated by dividing V_{max} by K_m
*$p<0.01$ from the control group by Student's *t*-test

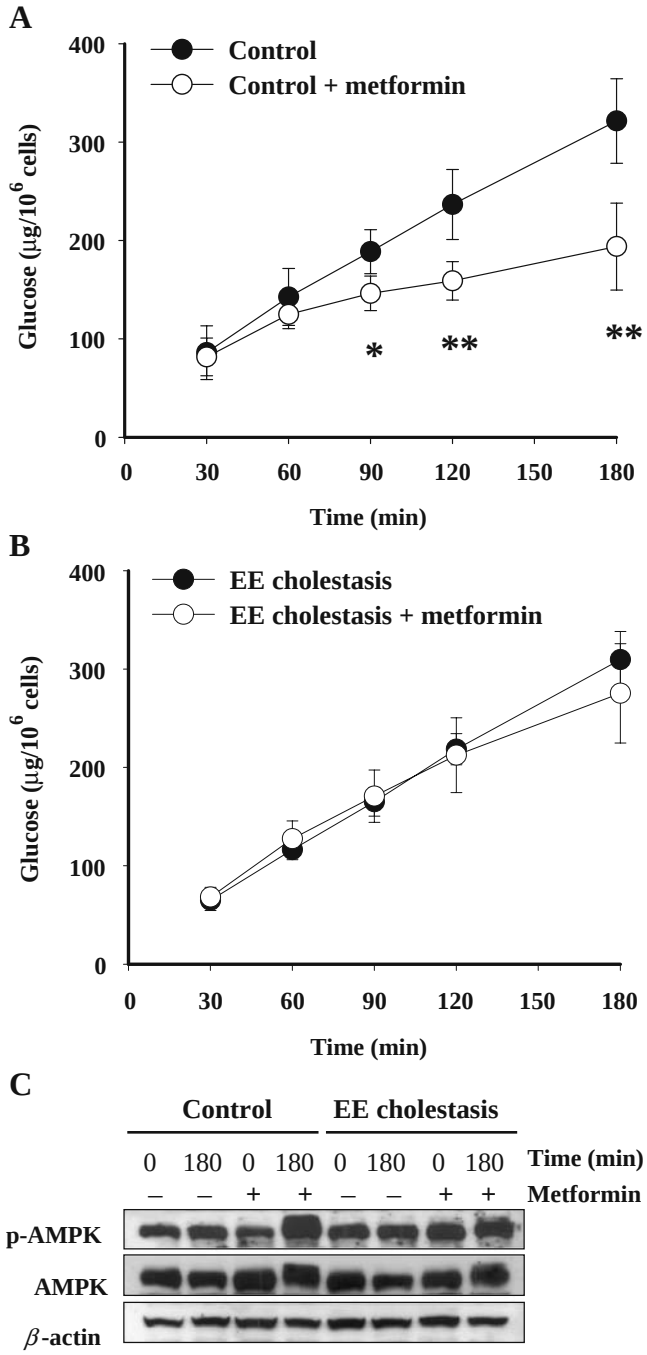

Fig. 7. Effect of metformin on glucose production in primary hepatocytes from control rats (**A**) and EE cholestatic rats (**B**), and phosphorylation of AMPK (*p-AMPK*; **C**). Hepatocytes from control rats and EE cholestatic rats were treated with (i.e., + metformin, *empty circles*) or without (i.e., *filled circles*) metformin (2 mM). Each data value in **A**, **B** is represented as the mean±SD of three experiments (n=4). *p<0.01, **p<0.001 from the without metformin group by Student's t-test.

cation transporters (OCTs) (36). OCT family members such as OCT1, OCT2, and OCT3 have been identified, and their physiological and pharmacokinetic roles have been evaluated (36, 37). Oct1 is expressed abundantly in the liver and kidney (38) of rats, whereas Oct2 is expressed predominantly in the kidney, but not in the liver (39). These transporters are localized to the basolateral membranes of renal proximal tubules. Oct3 is expressed predominantly in the placenta, but has also been detected in the intestine, heart, brain, lung, and very weakly in the kidney (40). In the renal proximal tubules of rats, Oct1 and Oct2 are considered to mediate the basolateral uptake of various cationic compounds.

Experimental intrahepatic cholestasis induced by 17α-ethynylestradiol (EE) treatment is a widely used animal model of the clinical counterparts of oral contraceptive-induced cholestasis, intrahepatic cholestasis of pregnancy, and cholestasis induced by postmenopausal hormone replacement therapy (17).

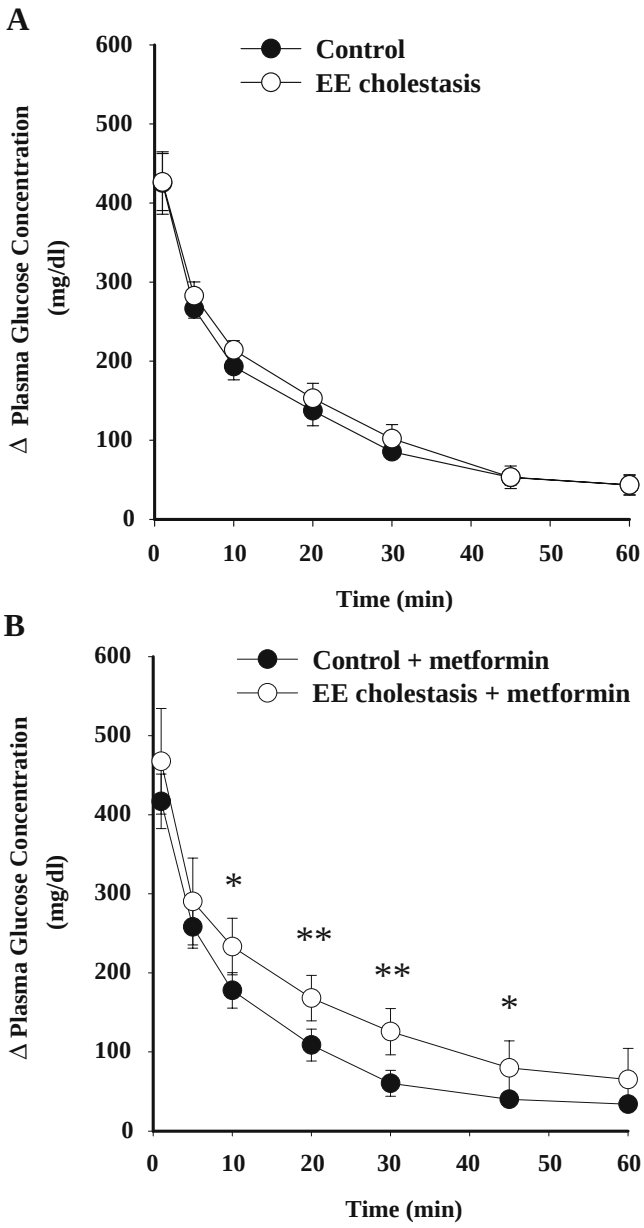

Fig. 8. Change in plasma glucose concentrations (presented as Δ Plasma Glucose Concentration) after the intravenous glucose tolerance test (40% D-glucose 1 g/kg) in the control and EE cholestatic rats without (**A**) or with (**B**) pretreatment of metformin (*iv*, 30 mg/kg). Each data value is represented as the mean±SD (n=5). *p<0.05, **p<0.01 from the control group by Student's t-test.

In the present study, we examined the effect of EE cholestasis on the pharmacokinetics of the organic cation drug, metformin, in association with the expressional change of Oct1 and Oct2 in rat liver and kidney. Previous transport studies demonstrated that metformin is a substrate for OCT1 and OCT2, but not for OCT3 (27). Down-regulation of Mrp2 is known to cause cholestatic liver injury *via* inhibition of biliary excretion of bile acids (20,21). In the present study, mRNA levels of hepatic Mrp2 (47%) as well as hepatic Oct1 (29%) were significantly reduced in EE cholestatic rats compared to control rats (Fig. 3A). In the case of hepatic Oct1, the decrease in protein level with EE cholestasis (69% of control) was comparable to that of mRNA (Fig. 4). The reduction of hepatic expression of Oct1 appears to be a general outcome of experimental cholestasis, because a similar reduction that was induced by bile duct ligation (BDL) (41) or intraperitoneal injection of lipopolysaccharide (LPS) was also observed in rats with experimental cholestasis (42). An elevated hepatic level of bile acids, as well as diminished bile flow, appear to be responsible for the reduction of Oct1 in the BDL model (43). However, EE cholestasis in the present study is characterized by the reduction of bile flow (Table I) and bile acid synthesis, with only a mild increase in bile acids in the serum, but not within hepatocytes (18,35,44), and minor morphological changes in hepatocytes with evidence of an increased mitotic index (17, 34). Elucidation of the factors and mechanisms that regulate the expression of Oct1 in each cholestasis model will require further investigation.

Hepatic uptake is one of the main processes that determine the intrahepatic concentration of drugs. Hepatic uptake clearance (CL_{uptake}) of metformin *in vivo* was decreased to about 28% of control in EE cholestatic rats (Table III), which is consistent with the fact that metformin is a substrate of Oct1 and the expression of the transporter was significantly reduced by EE cholestasis (Figs. 3A and 4). Decreased hepatic uptake of metformin was also reported for Oct1 knockout mice, supporting the principal involvement of Oct1 in the uptake (26).

The mRNA expression of Oct1 and Oct2 in the kidney was significantly depressed by EE cholestasis (Fig. 3B). The decrease in Oct2 mRNA was remarkable compared with that in Oct1 mRNA, suggesting that Oct2 was more sensitive to EE cholestasis. Western blot analysis also revealed the suppressed expression of Oct2, but not of Oct1 (Fig. 5). A similar result was reported for BDL-induced cholestatic rats, in which a sufficient increase in Oct1 mRNA expression in the kidney was not associated with significant changes in the Oct1 protein level (41). As a consequence of the down-regulation of renal Oct2, CL_{uptake} of metformin in the kidney was decreased to about 62% of control in EE cholestatic rats (Table III). Down-regulation of renal Oct2 as well as hepatic Oct1, and a subsequent reduced distribution of metformin to the liver and kidney, appear to be responsible for the 43% decrease in V_{dss} of the drug by EE cholestasis (Table II).

It was recently reported that the expression of Oct2 was up-regulated by testosterone and down-regulated by estradiol in rats (45), and that the lowered plasma level of testosterone was responsible for the decreased Oct2 expression (46). It was proposed that testosterone induced the expression of Oct2, but not of Oct1 and Oct3, *via* the androgen receptor-mediated transcriptional pathway (47). Consistent with these reports, the serum testosterone level in the present study was significantly reduced in EE cholestatic rats (1.6 vs 0.08 ng/ml, Table I). However, testosterone dependency should await further careful study, because testosterone-independent Oct2 suppression in the kidney has been reported recently in uranyl nitrate-induced acute renal failure rats (48). In that sense, the factors and underlying mechanisms that regulate the expression of Oct2 will require further study.

EE cholestasis in the present study exhibited a 30% increase in the AUC and a 21% decrease in the CL of metformin (Fig. 2 and Table II). Based on the literature (25), renal Oct2, compared with hepatic Oct1, should be more important to the plasma pharmacokinetics of metformin: only 0.5% of the *iv* dose is eliminated *via* biliary excretion, and the rest is eliminated *via* urinary excretion (26). Sambol *et al.* (49) suggested that the pharmacokinetics of metformin is related to renal function. Consistent with these reports, the decrease in systemic clearance (CL) in the EE cholestatic rats had nothing to do with nonrenal clearance (CL_{NR}), and could be explained solely by the decrease in renal clearance (CL_R; Table II). The glomerular filtration rate (GFR), which was estimated by the creatinine clearance, was not changed by EE cholestasis (Table II). Therefore, down-regulation of renal Oct2, not of GFR, appears to be responsible for the decrease of CL_R and CL of metformin in EE cholestatic rats.

It was recently reported that some diabetic patients did not respond sufficiently to metformin, even under approved dosage conditions (50). In the previous report (27), it was suggested that an uptake transporter, OCT1, played a key role in the antidiabetic efficacy of metformin. Although the plasma concentration profile of metformin was not significantly different between $Oct1^{+/+}$ mice and $Oct1^{-/-}$ mice, OCT1 genetic variants are known to be associated with different responses to metformin in healthy human volunteers (27). Consistent with this report, hepatic concentration of metformin was reduced in EE cholestatic rats following *iv* administration of metformin (Table III) and the maximum *in vitro* uptake velocity (V_{max}) of metformin into hepatocytes was decreased 7-fold by EE cholestasis, probably due to reduced Oct1 expression (Fig. 6 and Table IV). In line with decreased hepatic uptake of metformin, distinct inhibition of glucagon-stimulated glucose production in control hepatocytes (i.e., 40% for 180 min, Fig. 7A) disappeared in EE cholestatic hepatocytes (Fig. 7B). These *in vitro* results are consistent with the *in vivo* IVGTT data (Fig. 8).

The glucose tolerance test has been frequently used in investigating the effect of metformin on glucose utilization after glucose ingestion (27,51). We conducted the IVGTT study of metformin according to the design of a previous paper (27). Because metformin does not induce hypoglycemia under normal conditions, the blood glucose reduction effect of metformin was investigated under the administration of glucose. Metformin pretreatment caused plasma glucose levels to fall more rapidly in control rats than in EE cholestatic rats during the IVGTT, with a resultant decrease in the AUC of Δ Plasma Glucose Concentration (Fig. 8B). According to the previous report (52), the predominant mechanism of metformin action is to suppress hepatic glucose production rather than to enhance insulin sensitivity in peripheral tissue. Therefore, a different effect of metformin

in control and EE cholestatic rats *in vivo* might represent the different suppression of metformin against hepatic glucose production.

Zhou G., *et al*. (3) reported that activation of AMPK by metformin leads not only to the lowering of hepatic glucose production, but also to a reduction of hepatic steatosis and an increase in insulin sensitivity. When the phosphorylation level of AMPK in primary hepatocytes after the glucose production study for 180 min was detected by Western blot, metformin stimulated AMPK phosphorylation in control hepatocytes, but not in EE cholestatic hepatocytes (Fig. 7C).

In conclusion, the antidiabetic effect of metformin, an Oct1 substrate drug, is expected to diminish in diabetic patients with EE cholestasis, due to impaired hepatic uptake of the drug *via* the transporter. Since a variety of substrates are subjected to being transported *via* OCTs, the regulation may have broader implications for the understanding of the altered pharmacokinetics and pharmacologic effects of relevant substrate drugs of the transporters in experimental, as well as in clinical, estrogen-induced cholestasis.

ACKNOWLEDGEMENTS

This work was supported by the Korea Science and Engineering Foundation (KOSEF) through the National Research Lab. The program is funded by the Ministry of Science and Technology (no. R0A-2006-000-10190-0).

REFERENCES

1. D. Kirpichnikov, S. I. McFarlane, and J. R. Sowers. Metformin: an update. *Ann. Intern. Med.* **137**:25–33 (2002).
2. M. B. Davidson, and A. L. Peters. An overview of metformin in the treatment of type 2 diabetes mellitus. *Am. J. Med.* **102**:99–110 (1997), doi:10.1016/S0002-9343(96)00353-1.
3. G. Zhou, R. Myers, Y. Li, Y. Chen, X. Shen, J. Fenyk-Melody, M. Wu, J. Ventre, T. Doebber, N. Fujii, N. Musi, M. F. Hirshman, L. J. Goodyear, and D. E. Moller. Role of AMP-activated protein kinase in mechanism of metformin action. *J. Clin. Invest.* **108**(8):1105–1107 (2001).
4. W. Abbud, S. Habinowski, J. Z. Zhang, J. Kendrew, F. S. Elkairi, B. E. Kemp, L. A. Witters, and F. Ismail-Beigi. Stimulation of AMP-activated protein kinase (AMPK) is associated with enhancement of Glut1-mediated glucose transport. *Arch. Biochem. Biophys.* **380**:347–352 (2000), doi:10.1006/abbi.2000.1935.
5. A. Woods, S. R. Johnstone, K. Dickerson, F. C. Leiper, L. G. Fryer, D. Neumann, U. Schlattner, T. Wallimann, M. Carlson, and D. Carling. LKB1 is the upstream kinase in the AMP-activated protein kinase cascade. *Curr. Biol.* **13**:2004–2008 (2003), doi:10.1016/j.cub.2003.10.031.
6. R. J. Shaw, K. A. Lamia, D. Vasquez, S. H. Koo, N. Bardeesy, R. A. Depinho, M. Montminy, and L. C. Cantley. The kinase LKB1 mediates glucose homeostasis in liver and therapeutic effects of metformin. *Science.* **310**:1642–1646 (2005), doi:10.1126/science.1120781.
7. P. V. Katakam, M. R. Ujhelyi, M. Hoenig, and A. W. Miller. Metformin improves vascular function in insulin-resistant rats. *Hypertension*. **35**:108–112 (2000).
8. H. Z. Lin, S. Q. Yang, C. Chuckaree, F. Kuhakda, G. Ronnet, and A. M. Diehl. Metformin reverses fatty liver disease in obese, leptin-deficient mice. *Nat. Med.* **6**:998–1003 (2000), doi:10.1038/79697.
9. M. B. Schneider, H. Matsuzaki, J. Haorah, A. Ulrich, J. Standop, X. Z. Ding, T. E. Adrian, and R. M. Pour. Prevention of pancreatic cancer induction in hamsters by metformin. *Gastroenterology.* **120**:1263–1270 (2001), doi:10.1053/gast.2001.23258.
10. J. P. Baillargeon, M. J. Iuorno, and J. E. Nestler. Insulin sensitizers for polycystic ovary syndrome. *Clin. Obstet. Gynecol.* **46**:325–340 (2003), doi:10.1097/00003081-200306000-00011.
11. J. A. Rowan, W. M. Hague, W. Gao, M. R. Battin, M. P. Moore, and MiG Trial Investigators. Metformin *versus* insulin for the treatment of gestational diabetes. *N. Engl. J. Med.* **358**(19):2003–2015 (2008), doi:10.1056/NEJMoa0707193.
12. G. Hawthorne. Metformin use and diabetic pregnancy—has its time come? *Diabet. Med.* **23**:223–227 (2006), doi:10.1111/j.1464-5491.2006.01856.x.
13. T. Laatikainen, and E. Ikonen. Fetal prognosis in obstetric hepatosis. *Ann. Chir. Gynaecol. Fenn.* **64**:155–164 (1975).
14. M. Savander, A. Ropponen, K. Avela, N. Weerasekera, B. Cormand, M. L. Hirvioja, S. Riikonen, O. Ylikorkala, A. E. Lehesjoki, C. Williamson, and K. Aittomäki. Genetic evidence of heterogeneity in intrahepatic cholestasis of pregnancy. *Gut*. **52**:1025–1029 (2003), doi:10.1136/gut.52.7.1025.
15. M. L. Eloranta, S. Heinonen, T. Mononen, and S. Saarikoski. Risk of obstetric cholestasis in sisters of index patients. *Clin. Genet.* **60**:42–45 (2001), doi:10.1034/j.1399-0004.2001.600106.x.
16. P. L. Jansen, M. Muller, and E. Sturm. Genes and cholestasis. *Hepatology.* **34**:1067–1074 (2001), doi:10.1053/jhep.2001.29625.
17. E. A. Rodriguez-Garay. Cholestasis: human disease and experimental animal models. *Ann. Hepatol.* **2**:150–158 (2003).
18. R. Bossard, B. Stieger, B. O'Neill, G. Fricker, and P. Meier. Ethynylestradiol treatment induces multiple canalicular membrane transport alterations in rat liver. *J. Clin. Invest.* **1**:2714–2720 (1993), doi:10.1172/JCI116511.
19. D. Micheline, J. Emmanuel, and E. Serge. Effect of ursodeoxycholic acid on the expression of the hepatocellular bile acid transporters (Ntcp and Bsep) in rats with estrogen-induced cholestasis. *J. Pediatr. Gastroenterol. Nutr.* **35**:185–191 (2002), doi:10.1097/00005176-200208000-00015.
20. M. Trauner, M. Arrese, C. J. Soroka, M. Ananthanarayanan, T. A. Koeppel, S. F. Schlosser, F. J. Suchy, D. Keppler, and J. L. Boyer. The rat canalicular conjugate export pump (mrp2) is down-regulation in intrahepatic and obstructive cholestasis. *Gastroentreology.* **113**:255–264 (1997), doi:10.1016/S0016-5085(97)70103-3.
21. F. A. Crocenzi, E. J. Sánchez Pozzi, J. M. Pellegrino, C. O. Favre, E. A. Rodríguez Garay, A. D. Mottino, R. Coleman, and M. G. Roma. Beneficial effects of silymarin on estrogen-induced cholestasis in the rat: a study *in vivo* and in isolated hepatocyte couplets. *Hepatology*. **34**:329–339 (2001), doi:10.1053/jhep.2001.26520.
22. M. L. Ruiz, S. S. Villanueva, M. G. Luquita, M. Vore, A. D. Mottino, and V. A. Catania. Ethynylestradiol increases expression and activity of rat liver MRP3. *Drug. Metab. Dispos.* **34**(6):1030–1034 (2006).
23. A. Geier, C. G. Dietrich, T. Gerloff, J. Haendly, G. A. Kullak-Ublick, B. Stieger, P. J. Meier, S. Matern, and C. Gartung. Regulation of basolateral organic anion transporters in ethynylestradiol-induced cholestasis in the rat. *Biochim. Biophys. Acta*. **1609**:87–94 (2003), doi:10.1016/S0005-2736(02)00657-0.
24. J. M. Lee, M. Trauner, C. J. Soroka, B. Stieger, P. J. Meier, and J. L. Boyer. Expression of the bile salt export pump is maintained after chronic cholestasis in the rat. *Gastroenterology.* **118**:163–172 (2000), doi:10.1016/S0016-5085(00)70425-2.
25. N. Kimura, S. Masuda, Y. Tanihara, H. Ueo, M. Okuda, T. Katsura, and K. Inui. Metformin is a superior substrate for renal organic cation transporter OCT2 rather than hepatic OCT1. *Drug Metab. Pharmacokinet.* **20**:379–386 (2005), doi:10.2133/dmpk.20.379.
26. D. S. Wang, J. W. Jonker, Y. Kato, H. Kusuhara, A. H. Schinkel, and Y. Sugiyama. Involvement of organic cation transporter 1 in hepatic and intestinal distribution of metformin. *J. Pharmacol. Exp. Ther.* **302**:510–515 (2002), doi:10.1124/jpet.102.034140.
27. Y. Shu, S. A. Sheardown, C. Brown, R. P. Owen, S. Zhang, R. A. Castro, A. G. Ianculescu, L. Yue, J. C. Lo, E. G. Burchard, C. M. Brett, and K. M. Giacomini. Effect of genetic variation in the organic cation transporter 1 (OCT1) on metformin action. *J. Clin. Invest.* **117**:1422–1431 (2007), doi:10.1172/JCI30558.
28. I. S. Song, H. J. Shin, E. J. Shim, I. S. Jung, W. Y. Kim, J. H. Shon, and J. G. Shin. Genetic variants of the organic cation transporter 2 influence the disposition of metformin. *Clin. Pharmacol. Ther.* **83**:273–280 (2008), doi:10.1038/sj.clpt.6100275.

29. W. L. Chiou. Critical evaluation of potential error in pharmacokinetic studies using the linear trapezoidal rule method of the calculation of the area under the plasma level-time curve. *J. Pharmacokinet. Biophama.* **6**(6):539–549 (1978), doi:10.1007/BF01062108.
30. M. Gibaldi, and D. Perrier. *Pharmacokinetics vol. 2*. Marcel-Dekker, New York, 1982, pp. 145–188.
31. E. van Vliet, E. Aronica, S. Redeker, N. Marchi, M. Rizzi, A. Vezzani, and J. Gorter. Selective and persistent upregulation of mdr1b mRNA and P-glycoprotein in the parahippocampal cortex of chronic epileptic rats. *Epilepsy Res.* **60**:203–213 (2004), doi:10.1016/j.eplepsyres.2004.06.005.
32. Y. H. Han, S. J. Chung, and C. K. Shim. Canalicular membrane transport is primarily responsible for the difference in hepatobiliary excretion of triethyl methyl ammonium and tributyl methyl ammonium in rats. *Drug Metab. Dispos.* **27**(8):872–879 (1999).
33. J. Ma, Z. Ma, J. Wang, R. W. Miline, D. Xu, A. K. Davey, and A.M. Evans. Isosteviol reduces plasma glucose levels in the intravenous glucose tolerance test in Zucker diabetic fatty rats. *Diabetes Obes. Metab.* **9**:597–599 (2007), doi:10.1111/j.1463-1326.2006.00630.x.
34. N. R. Koopen, S. M. Post, H. Wolters, R. Havinga, F. Stellaard, R. Boverhof, F. Kuipers, and H. M. Princen. Differential effects of 17alpha-ethinylestradiol on the neutral and acidic pathways of bile salt synthesis in the rat. *J. Lipid. Res.* **40**(1):100–108 (1999).
35. F. R. Simon, J. Fortune, M. Iwahashi, C. Gartung, A. Wolkoff, and E. Sutherland. Ethynylestradiol cholestasis involves alterations in expression of liver sinusoidal transporters. *Am. J. Physiol.* **271**(6 Pt 1):G1043–G1052 (1996).
36. J. W. Jonker, and A. H. Schinkel. Pharmacological and physiological functions of the polyspecific organic cation Transporters: OCT1, 2, and 3 (SLC22A1–3). *J. Pharmacol. Exp. Ther.* **308**:2–9 (2004), doi:10.1124/jpet.103.053298.
37. K. Inui, S. Masuda, and H. Saito. Cellular and molecular aspects of drug transport in the kidney. *Kidney Int.* **58**:944–958 (2000), doi:10.1046/j.1523-1755.2000.00251.x.
38. D. Gründemann, V. Gorboulev, S. Gambaryan, M. Veyhl, and H. Koepsell. Drug excretion mediated by a new prototype of polyspecific transporter. *Nature*. 372:549–552 (1994), doi:10.1038/372549a0.
39. M. Okuda, H. Saito, Y. Urakami, M. Takano, and K. Inui. cDNA cloning and functional expression of a novel rat kidney organic cation transporter, OCT2. *Biochem. Biophys. Res. Commun.* **224**:500–507 (1996), doi:10.1006/bbrc.1996.1056.
40. R. Kekuda, P. D. Prasad, X. Wu, H. Wang, Y. J. Fei, F. H. Leiback, and V. Ganapathy. Cloning and functional characterization of a potential-sensitive, polyspecific organic cation transporter (OCT3) most abundantly expressed in placenta. *J. Biol. Chem.* **273**:15971–15979 (1998), doi:10.1074/jbc.273.26.15971.
41. G. U. Denk, C. J. Soroka, A. Mennone, H. Koepsell, U. Beuers, and J. L. Boyer. Down-regulation of the organic cation transporter 1 of rat liver in obstructive cholestasis. *Hepatology.* **39**:1382–1389 (2004), doi:10.1002/hep.20176.
42. N. J. Cherrington, A. L. Slitt, N. Li, and C. D. Klaassen. Lipopolysaccharide-mediated regulation of hepatic transporter mRNA levels in rats. *Drug. Metab. Dispos.* **32**:734–741 (2004).
43. C. Stedman, G. Robertson, S. Coulter, and C. Liddle. Feed-forward regulation of bile acid detoxification by CYP3A4. *J. Biol. Chem* **279**:11336–11343 (2004), doi:10.1074/jbc.M310258200.
44. R. A. Davis, and F. Kern Jr. Effects of ethynylestradiol and phenobarbital on bile acid synthesis and biliary bile acid and cholesterol excretion. *Gastroenterology.* **70**(6):1130–1135 (1976).
45. Y. Urakami, M. Okuda, H. Saito, and K. Inui. Hormonal regulation of organic cation transporter OCT2 expression in rat kidney. *FEBS Lett.* **473**:173–176 (2000), doi:10.1016/S0014-5793(00)01525-8.
46. L. Ji, S. Masuda, H. Saito, and K. Inui. Down-regulation of rat organic cation transporter rOCT2 by 5/6 nephrectomy. *Kidney Int.* **62**:514–524 (2002), doi:10.1046/j.1523-1755.2002.00464.x.
47. J. Asaka, T. Terada, M. Okuda, T. Katsura, and K. Inui. Androgen receptor is responsible for rat organic cation transporter 2 gene regulation but not for rOCT1 and rOCT3. *Pharm. Res.* **23**:697–704 (2006), doi:10.1007/s11095-006-9665-2.
48. W. S. Shim, J. H. Park, S. J. Ahn, L. Han, Q. R. Jin, H. Li, M. K. Choi, D. D. Kim, S. J. Chung, and C. K. Shim. Testosterone-independent down-regulation of Oct2 in the kidney medulla from a uranyl nitrate-induced rat model of acute renal failure: Effects on distribution of a model organic cation, tetraethyl ammonium. *J. Pharm. Sci.*(2008), doi:10.1002/jps.21442.
49. N. C. Sambol, J. Chiang, E. T. Lin, A. M. Goodman, C. Y. Liu, L. Z. Benet, and M. G. Cogan. Kidney function and age are both predictors of pharmacokinetics of metformin. *J. Clin. Pharmacol.* **35**(11):1094–1102 (1995).
50. E. Shikata, R. Yamamoto, H. Takane, C. Shigemasa, T. Ikeda, K. Otsubo, and I. Ieiri. Human organic cation transporter (OCT1 and OCT2) gene polymorphisms and therapeutic effects of metformin. *J. Hum. Genet.* **52**(2):117–122 (2007), doi:10.1007/s10038-006-0087-0.
51. F. Féry, L. Plat, and E. O. Balasse. Effects of metformin on the pathways of glucose utilization after oral glucose in non-insulin-dependent diabetes mellitus patients. *Metabolism*. **46**(2):227–33 (1997), doi:10.1016/S0026-0495(97)90307-3.
52. K. Cusi, A. Consoli, and R. A. DeFronzo. Metabolic effects of metformin on glucose and lactate metabolism in noninsulin-dependent diabetes mellitus. *J. Clin. Endocrinol. Metab.* **81**(11):4059–4067 (1996), doi:10.1210/jc.81.11.4059.